

Rényi Entropy Singularities as Signatures of Topological Criticality in Coupled Photon-Fermion Systems

F. P. M. Méndez-Córdoba,^{1,*} J. J. Mendoza-Arenas,¹ F. J. Gómez-Ruiz,^{2,1} F. J. Rodríguez,¹ C. Tejedor,³ and L. Quiroga¹

¹*Departamento de Física, Universidad de Los Andes, A.A. 4976, Bogotá, Colombia*

²*Donostia International Physics Center, E-20018 San Sebastián, Spain*

³*Departamento de Física Teórica de la Materia Condensada and Condensed Matter Physics Center (IFIMAC), Universidad Autónoma de Madrid, Madrid 28049, Spain*

We establish the relation between topological phase (TP) transitions and quantum entropy singularities in a Kitaev chain embedded in a cavity. Even though both the von Neumann and Rényi entanglement entropies between light and matter sub-systems display singularities at the TP transition, we show that remarkably the Rényi entropy is analytically connected to the measurable photon Fano factor. Thus, we put forward a path to experimentally access the control and detection of a TP phase transition via a Rényi entropy analysis.

Introduction.— The understanding of quantum light and matter in the strongly coupling regime has been an intense area of research both theoretically and experimentally in the last few years. Hybrid photonic technologies for control of complex systems have been constantly improving, now acting as cornerstones for quantum simulations in cutting-edge platforms such as optical lattices. Namely, trapped ions are subjected to high control by laser beams allowing the manipulation of the main system parameters [1–5]. Strong light-matter couplings have been generated in superfluid and Bose-Einstein gases embedded in cavities now available to study systems with exquisitely tailored properties [6–9]. Furthermore, the analysis of light-controlled condensed matter systems has led to predictions of a rich variety of phenomena, including the enhancement of electron-photon superconductivity by cavity mediated fields [10–15]. Experimentally, new physical features as well as control opportunities in the ultrastrong and deep-strong coupling regimes, where coupling strengths are comparable to or larger than sub-system energies, have been observed recently using circuit quantum electrodynamics microwave cavities [16, 17].

Motivated by these remarkable advances, we are encouraged to establish new feasible scenarios for the detection and control of non-local correlated features in solid-state setups such as topological materials. A great deal of attention has been recently devoted to assessing non-local Majorana fermion quasiparticles in chains with strong spin-orbit coupling disposed over an s-wave superconductor [18–21]. Majorana fermions, as topological quasi-particles in solid-state environments, have been widely searched due to their unconventional properties against local decoherence and hence for possible technological solutions to fault-tolerant quantum computing protocols [22–25]. Since the seminal work by Kitaev [26] where a one-dimensional spinless fermion chain was shown to feature Majorana physics, topological properties of hybrid semiconductor-superconductor systems [18–21] have been explored looking for the presence of

the so called Zero Energy Modes (ZEM) corresponding to quasiparticles localized at the boundaries of the chain. The fact that these quasiparticles have zero energy makes them potential candidates for the use of non-Abelian gate operations within 2D arrangements [27–31]. However, reported experimental results, that claimed to have detected those elusive quasiparticles, have been pretty much controversial up to date. The reported phenomena observed in those experiments could be caused by a variety of alternative competing effects [32]. Therefore, new experimental frames are highly desirable to find unambiguous signs of such quasiparticles.

An important question in this context is whether the topological phase transition of Majorana polaritons, for instance in a fermion chain embedded in a cavity [11], can be detected by optically accessing observables such as the mean number of photons, field quadratures or Fano factor (FF). In this paper, we report on an information-theoretic approach based on the analysis of Rényi entropy of order two (S_R) for connecting its singular behavior at the borderlines of the system phase diagram with the FF , clarifying more generally the role of topological phases hosted by cavity-fermion coupled systems. This approach allows us to link directly accessible microwave observables to quantum light-matter correlations [33–35]. Below, we will show that in a wide parameter coupling regime the cavity state is faithfully represented by a Gaussian state (GS). Within this description, measurements of the Fano parameter and single-mode quadrature amplitudes yield directly to assessing the Rényi entropy between light and matter sub-systems. We show that, as a result of the topological phase transition, relevant observables of the system, namely photon statistical properties and quantum (the von Neumann (S_N) and Rényi (S_R)) entropies, inherit the singular behavior of Majorana polaritons at the borderlines of the phase diagram of the system, as signaled by the non-monotonic non-local correlations in the fermion chain.

Photon-Fermion Model.— We consider a Kitaev chain

embedded in a single-mode microwave cavity described by the Hamiltonian

$$\hat{\mathcal{H}} = \hat{\mathcal{H}}_C + \hat{\mathcal{H}}_K + \hat{\mathcal{H}}_{\text{Int}}. \quad (1)$$

Here, $\hat{\mathcal{H}}_C = \omega \hat{a}^\dagger \hat{a}$ is the Hamiltonian describing the microwave single-mode cavity, with \hat{a} (\hat{a}^\dagger) the annihilation (creation) microwave photon operator and ω is the energy of the cavity; we set the energy scale by taking $\omega = 1$. The isolated open-end Kitaev chain Hamiltonian $\hat{\mathcal{H}}_K$ is given by

$$\begin{aligned} \hat{\mathcal{H}}_K = & -\frac{\mu}{2} \sum_{j=1}^L [2\hat{c}_j^\dagger \hat{c}_j - 1] \\ & -t \sum_{j=1}^{L-1} [\hat{c}_j^\dagger \hat{c}_{j+1} + \hat{c}_{j+1}^\dagger \hat{c}_j] + \Delta \sum_{j=1}^{L-1} [\hat{c}_j \hat{c}_{j+1} + \hat{c}_{j+1}^\dagger \hat{c}_j^\dagger]. \end{aligned} \quad (2)$$

where \hat{c}_j (\hat{c}_j^\dagger) is the annihilation (creation) operator of spinless fermions at site $j = 1, \dots, L$, μ is the chemical potential, t is the hopping amplitude between nearest-neighbor sites (we assume $t \geq 0$ without loss of generality) and Δ is the nearest-neighbor superconducting induced pairing interaction. The Kitaev model features two phases: a topological phase and a trivial one. In the former the Majorana ZEM emerge, which occurs whenever $|\mu| < \pm 2\Delta$ for the symmetric hopping-pairing Kitaev Hamiltonian, i.e. $t = \Delta$, the case we restrict ourselves from now on [26, 28]. Additionally, the general interaction Hamiltonian is given by [11]

$$\hat{\mathcal{H}}_{\text{Int}} = \left(\frac{\hat{a}^\dagger + \hat{a}}{\sqrt{L}} \right) \left[\lambda_0 \sum_{j=1}^L \hat{c}_j^\dagger \hat{c}_j + \frac{\lambda_1}{2} \sum_{j=1}^{L-1} (c_j^\dagger c_{j+1} + \hat{c}_{j+1}^\dagger \hat{c}_j) \right]. \quad (3)$$

Here for the light-matter interaction, we shall consider a general case which incorporates both on-site (λ_0) as well as hopping-like (λ_1) terms (without loss of generality we will assume $\lambda_0, \lambda_1 > 0$). In Ref. [11], a typical value of the on-site chain-cavity coupling, $\lambda_0 \simeq 0.1\omega$ was estimated for a fermion chain length of $L = 100$ sites. Note that the whole chain is assumed to be coupled to the same cavity field.

Mean-Field Approach.— In order to gain physical insights on how the original topological phase of the Kitaev chain is modified by its coupling to a cavity, we start by performing a Mean-Field (MF) its. Although we focus the MF analysis for a chain with periodic boundary conditions, the relations we will discuss in this section are indeed useful guides for interpreting the quasi-exact results obtained by Density Matrix Renormalization Group (DMRG) numerical simulations in chains with open boundary conditions, as illustrated below.

We start by separating the cavity and the chain subsystems by describing their interaction as the mean effect of one sub-system over the other one. The resulting MF Hamiltonian is rewritten as $\hat{\mathcal{H}}_{\text{MF}} \approx \hat{\mathcal{H}}_C + \hat{\mathcal{H}}_K + \hat{\mathcal{H}}_{\text{Int}}^{\text{MF}}$;

where, the new interaction Hamiltonian is given by

$$\begin{aligned} \hat{\mathcal{H}}_{\text{Int}}^{\text{MF}} = & L(\lambda_1 D - \lambda_0 S_z) [\hat{X} - x] + \lambda_0 L \hat{X} \\ & + 2x \left[\lambda_0 \sum_{j=1}^L \hat{c}_j^\dagger \hat{c}_j + \frac{\lambda_1}{2} \sum_{j=1}^{L-1} (c_j^\dagger c_{j+1} + \hat{c}_{j+1}^\dagger \hat{c}_j) \right]. \end{aligned} \quad (4)$$

Here, we define $\hat{X} = (\hat{a} + \hat{a}^\dagger)/2\sqrt{L}$, $x = \langle \hat{X} \rangle$, $S_z = 1 - \frac{2}{L} \sum_j \langle \hat{c}_j^\dagger \hat{c}_j \rangle$, and $D = \sum_j \langle \hat{c}_j^\dagger \hat{c}_{j+1} + \hat{c}_{j+1}^\dagger \hat{c}_j \rangle / L$, where expectation values are taken with respect to the photon-fermion ground state. The resulting Hamiltonian is that of a displaced harmonic oscillator, with photon number $\langle \hat{a}^\dagger \hat{a} \rangle \equiv \langle \hat{n} \rangle = Lx^2$, and a Kitaev chain with effective chemical potential $\mu_{\text{eff}} \equiv \mu - 2\lambda_0 x$ and hopping interaction $\Delta_{\text{eff}} \equiv \Delta - \lambda_1 x$ (see Supplementary Material (SM) [36]).

The minimization of the MF Hamiltonian expected value, $\partial \langle \hat{\mathcal{H}}_{\text{MF}} \rangle / \partial x = 0$, yields to:

$$\lambda_0 S_z = \lambda_0 + \lambda_1 D + 2\omega x, \quad (5)$$

which shows the interdependence of the cavity and chain states parameters. As long as $x \in [-\frac{2\lambda_0 + \lambda_1}{2\omega}, 0]$, the effective MF renormalized Kitaev parameters turns out to be $\mu_{\text{eff}} \geq \mu$ and $\Delta_{\text{eff}} \geq \Delta$. By choosing $\lambda_1 = 0$, it is easy to see that x will be related to the magnetization in the equivalent transverse Ising chain [37–40], while when choosing $\lambda_0 = 0$, x will be associated to the occupancy of first neighbor non-local Majorana fermions in the Kitaev chain [22].

Phase Diagram.— The ground state of the system has been obtained by performing DMRG simulations in a matrix product state description [41, 42], using the open-source TNT library [43, 44]. Notably, matrix product algorithms have been successfully applied to correlated systems embedded in a cavity [45, 46], as well as to different interacting systems in star-like geometries [47–50]. In the following analysis, we consider separately each kind of cavity-chain coupling term and we sweep over μ .

The topological phase of the chain will be assessed through the two end correlations Q , defined as $Q \equiv 2\langle \hat{c}_1 \hat{c}_L^\dagger + \hat{c}_L \hat{c}_1^\dagger \rangle$. For an infinite isolated Kitaev chain, its value is 1 in the topological phase while it goes to 0 in the trivial one. However, for finite sizes the value of Q takes on continuous values in between, leaving a value of 1 at the point of maximum correlations (cf. insets of Fig. 1). Whenever $Q > Q_{\text{Trigger}}$ the phase is said to be topological, where Q_{Trigger} was defined as the lowest Q that allows for ZEM to emerge in an isolated Kitaev chain with same Δ and L as the simulated case. For both types of couplings, second-order phase transitions arise in the composite light-matter model, a result for which DMRG and MF are in full agreement for a wide range of experimental coupling values (see SM [36]).

The phase diagram for the on-site coupling ($\lambda_0 \neq 0$ and $\lambda_1 = 0$) is presented in Fig. 1(a), whereas that for the hopping-like coupling ($\lambda_0 = 0$ and $\lambda_1 \neq 0$) is depicted

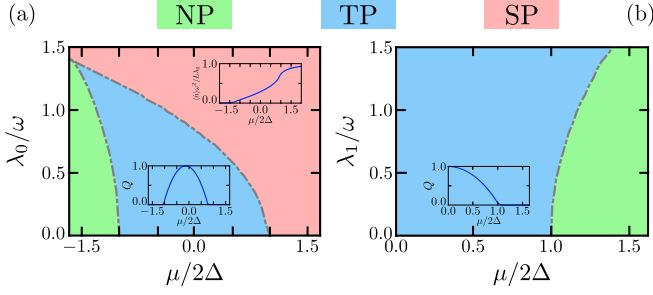


Figure 1. Photon-fermion phase diagrams. NP: normal phase, TP: topological phase and SP: super-radiant phase. (a) Chemical potential-like coupling. Upper inset: number of photons normalized by the expression obtained from MF. (b) Hopping-like coupling. The Kitaev-cavity parameters are $L = 100$ and $\Delta = 0.6\omega$. Lower insets in (a) and (b) depict the long-range Q correlation behavior when the respective coupling is set to 0.4ω

in Fig. 1(b). The relation in Eq. (5) fits successfully the numerical results with vanishing differences (see SM [36]).

We can summarize the effect of the λ_0 coupling in the phase diagram with the presence of three phases: a normal phase (NP) in both the cavity and the chain; a topological phase (TP) in the chain which allows super-radiance, and a trivial phase in the chain that possesses an asymptotic value of the number of photons in the cavity (SP) (cf. upper inset in Fig. 1(a); the normalized $\langle \hat{n} \rangle$ goes to 1 as we increase $\mu/2\Delta$). The critical points and the maximum of correlations move asymmetrically to lower values of the chemical potential as λ_0 increases due to the shift in μ_{eff} . The boundary between the topological phase and the asymptotically super-radiant phase is affected more dramatically causing the topological phase to vanish at $\lambda_0/\omega = 1.39 \pm 0.01$. After this point, for higher values of λ_0 , there will only be one interface between a non-radiant and a radiant phase, phases for which the ordering of the chain is trivial.

For the hopping-like photon-chain coupling case, the phase transition points are symmetrical with respect to $\mu \rightarrow -\mu$ since now $\mu_{\text{eff}} = \mu$ (for details see [36]). Furthermore, the whole area belonging to the topological phase can be characterized easily with the radiation properties in the cavity. The last feature is endorsed by the Q value and the number of photons from our DMRG results. Thus whenever the cavity resides in a super-radiant phase, the chain is in the topological phase and the mean number of photons acts as an order-like parameter that correlates well with the quantum state of the chain. Moreover, we find that the borderline between the super-radiant topological and the trivial phase shifts to the right as we increase λ_1 . This results in increased robustness of the topological phase since for an isolated chain its extension would be bounded by $\mu/2\Delta = \pm 1$. As a consequence, the interaction with the cavity could

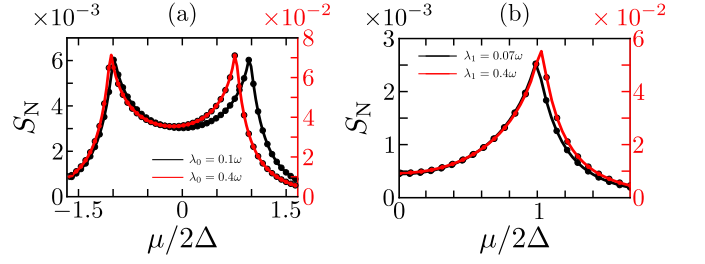


Figure 2. Von Neumann entropy S_N as a function of the chemical potential of the chain $\mu/2\Delta$ for any sub-system in the bipartite cavity-chain system. Symbols (lines) indicate DMRG (Gaussian) results. (a) Local photon-fermion couplings $\lambda_0 = 0.1\omega$ (weak coupling, black symbols and line) and $\lambda_0 = 0.4\omega$ (moderate coupling, red symbols and line). (b) Non-local photon-fermion coupling $\lambda_1 = 0.07\omega$ (weak coupling, black symbols and line) and $\lambda_1 = 0.4\omega$ (moderate coupling, red symbols and line). Other parameters are $L = 100$, $\omega = 1$ and $\Delta = 0.6\omega$

drive the chain into a topological phase, but this allowed enhancement is not limitless since second-order terms in the cavity energy $\omega \hat{a}^\dagger \hat{a}$ could become relevant for very strong λ_1 , destroying the superradiance [51]. In addition, as we increase the topological phase the maximum value of Q decreases, degrading the two ends correlations at high coupling values.

Von Neumann entropy, criticality and Gaussian states.— A result well beyond the MF analysis for this photon-fermion system is that phase transitions are associated with singularities in the quantum entropies for any sub-system, such as S_N and S_R [2, 44, 52], as shown in Fig. 2. Critical lines are obtained from the non-local Q -correlation behavior; those are fully consistent with results extracted from the second derivative of the energy and S_N (for further details see [36]). Moreover, the maximum non-local edge correlation $Q = 1$ coincides with the minimum S_N (compare the lower inset of Fig. 1(a) with Fig. 2(a)). For a free chain with the parameters assumed in Fig. 2, the phase transitions occur at $\mu/2\Delta = \pm 1$. Now, for a strongly coupled photon-fermion system ($\lambda_0 = 0.4\omega$ in Fig. 2(a)), they shift to $\mu/2\Delta = -1.03 \pm 0.02$ and $\mu/2\Delta = 0.76 \pm 0.02$. Thus, the chain topological phase region is reduced by the on-site like coupling to the cavity. Even more, the maximally-correlated state is shifted towards negative values of μ (inset Fig. 1(a)). Consistency with entropy singularities is shown for the hopping-like coupling in Fig. 2(b). The topological phase region gets enhanced by the cavity coupling with transitions now occurring at $\mu/2\Delta = \pm(1.03 \pm 0.02)$ ($\lambda_1 = 0.4\omega$ in Fig. 2(b)). The shift effect for both couplings at lower interaction parameters is less dramatic (Fig. 2 $\lambda_0 = 0.1\omega$ and $\lambda_1 = 0.07\omega$). In addition, we have observed that as Δ decreases, the shift increases (not shown). In any case, singularities in S_N

are intimately connected to the phase transition.

The MF analytical results provide an accurate description of the bulk expectation values in the chain, the mean number of cavity photons and the energy of the whole system. The MF description of the cavity involved a single coherent state, which is a good approximation for second-order expected values in bosonic terms. However, this effective description is unable to account for entanglement properties between sub-systems and higher interaction terms such as the FF . Remarkably, an accurate description of the reduced photon system density matrix is possible by means of a single mode GS. Any single-mode GS can be expressed in terms of a fictional thermal state on which squeezed (\hat{S}_ξ) and displacement (\hat{D}_α) operators act in the form:

$$\hat{\rho}_{\text{GS}} = \hat{D}_\alpha \hat{S}_\xi \frac{N \hat{a}^\dagger \hat{a}}{(1+N)^{a^\dagger a}} S_\xi^\dagger D_\alpha^\dagger, \quad (6)$$

where $\hat{D}_\alpha = \exp[\alpha \hat{a}^\dagger - \alpha^* \hat{a}]$ with $\alpha \in \mathbb{C}$, $\hat{S}_\xi = \exp[(\xi^*(\hat{a})^2 - \xi(\hat{a}^\dagger)^2)/2]$ where $\xi = re^{i\phi}$ is an arbitrary complex number with modulus r and argument ϕ , and N is the thermal state parameter [53]. Many of the properties of GS have been broadly studied [53–56] being one of the most outstanding the fact that it is fully characterized by its 2×2 covariance matrix and first moments of the field-quadrature canonical variables given by $\hat{q} = (\hat{a}^\dagger + \hat{a})/\sqrt{2}$ and $\hat{p} = i(\hat{a}^\dagger - \hat{a})/\sqrt{2}$. Furthermore, a well known fact is that S_N is maximized for a single-mode GS at given quadrature variances and it is simply expressed as $S_N = (N+1) \ln[N+1] - N \ln[N]$ [55].

In order to get the α , N , r , and ϕ Gaussian parameters, the covariance matrix and quadratures are numerically extracted from the corresponding expected values using ground state DMRG calculations. The imaginary part of α and ϕ must be 0 to reach the ground state [36], leading to $\alpha \in \mathbb{R}$ in the present case. The S_N can be analytically calculated for a GS [54, 57]. The results of S_N obtained from DMRG and GS calculations have an excellent agreement for different coupling values for a wide class of light-matter interactions and strengths, as shown in Fig. 2, thus confirming the adequacy of a GS photon description for the present photon-fermion system.

Rényi entropy and Fano factor.— The Rényi entropies, defined as $S_\alpha(\hat{\rho}) = (1-\alpha)^{-1} \ln[\text{tr}[\hat{\rho}^\alpha]]$ for a state $\hat{\rho}$, have been identified as powerful indicators of quantum correlations in multipartite systems [58]. The Von Neumann entropy S_N is retrieved as the Rényi entropy in the limit $\alpha \rightarrow 1$. It has also been established that the Rényi entropy of order $\alpha = 2$ is well adapted for extracting correlation information from GS. Thus, from now on we restrict ourselves to consider only $S_2(\rho) = -\ln[\text{tr}(\rho^2)]$ which we will simply note as S_R [2, 3, 24]. Specifically, S_R for a GS can be simply expressed in terms of the GS covariance matrix σ (see SM [36]) as $S_R = \frac{1}{2} \ln[\det(\sigma)]$.

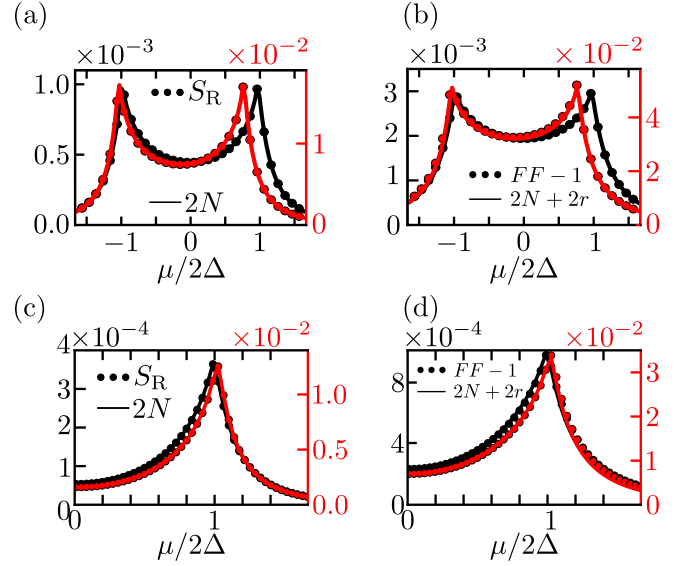


Figure 3. ((a), (c)) Rényi entropy S_R and ((b), (d)) Fano factor ($FF-1$) of the cavity state as a function of the chemical potential of the chain $\mu/2\Delta$. Symbols (lines) indicate DMRG (GS) results. (a)-(b) Local photon-fermion coupling, $\lambda_0 = 0.1\omega$ ($\lambda_1 = 0.4\omega$) black (red) symbols-lines. (c)-(d) Non-local photon-fermion coupling, $\lambda_1 = 0.07\omega$ ($\lambda_1 = 0.4\omega$) black (red) symbols-lines. Other parameters are $L = 100$, $\omega = 1$ and $\Delta = 0.6\omega$.

Next, we focus our attention on the photon FF , which is defined as $FF = \text{Var}(\hat{n})/\langle\hat{n}\rangle$, with $\text{Var}(\hat{n}) = \langle\hat{n}^2\rangle - \langle\hat{n}\rangle^2$. This value, turns out to be $FF = 1$ for a single coherent state (MF result); otherwise the cavity is either in a sub- ($FF < 1$) or super- ($FF > 1$) Poissonian state. We now argue that the GS approximation allows us to analytically work out a relation between the FF and the entanglement entropy S_R , raising them as both reliable and accessible indicators of phase transitions in composed photon-fermion systems.

For a cavity GS, the FF and the S_R can be analytically expressed as [53, 54, 57]:

$$FF = \frac{(N+1/2)^2 \cosh[4r] + (1+2N)e^{2r}\alpha^2 - 1/2}{(N+1/2) \cosh[2r] + \alpha^2 - 1/2}, \quad (7)$$

$$S_R = 2 \ln[1+N] + \ln \left[1 - \left(\frac{N}{1+N} \right)^2 \right]. \quad (8)$$

For both kinds of photon-fermion couplings, results obtained from these analytical expressions fit exactly the numerical ones extracted from full DMRG calculations. Assuming a GS, the inequalities $N, r \ll |\alpha|$ and $N, r \ll 1$, which allow to clearly see the connection between both quantities, are reliable and well justified for the range of parameters of experimental interest (see SM [36]). Keeping first order terms in r and N , in Eqs. (7) and (8), we finally get $FF = 1 + 2(r+N)$ and

$S_R = 2N$, from which a simple relationship between S_R , FF and the squeezing parameter r immediately follows as

$$S_R = FF - 2r - 1. \quad (9)$$

The validity of this important relation is illustrated in Fig. 3 regardless of the photon-fermion coupling type. In spite of the similar behavior through a topological phase transition (and corresponding analytical expressions for a GS) of von Neumann and Rényi entropies, it is important to note that an equivalent relation to that in Eq. (9) but involving S_N instead of S_R is hardly workable. Therefore, we stress the relevance of this connection between a theoretical quantum information entropy, S_R , and measurable photon field observables, FF and r .

Figs. 3(a)-(b) exhibit the behavior of different terms involved in Eq. (9) for the local photon-fermion coupling ($\lambda_0 = 0.1\omega$ and 0.4ω), and shows an excellent agreement between the results directly obtained from DMRG and those assuming a cavity GS. This validates Eq. (9), according to which $S_R + 2r$ and $FF - 1$ coincide. Very small deviations between GS and DMRG results at the topological phase transition are observed, for the stronger coupling value, but the locations of the singularities predicted by the analytical and numerical results coincide. On the other hand, Figs. 3(c)-(d) display similar results for a hopping like coupled system ($\lambda_1 = 0.07$ and 0.4) showing that GS results seem to slightly drift apart from the numerically exact DMRG ones.

We observe that the squeezing gets larger as the light-matter sub-systems become more entangled, at the critical point (note the behavior of the r parameter comparing the different curves in Fig. 3; see also SM [36]). In order to measure the squeezing parameter r , one can resort to a well known procedure in quantum optics by using homodyne detection techniques which has been recently extended to the microwave spectral region [59–61]. Thus, the FF behavior and its very close relation with S_R turn out to be reliable good indicators of entanglement for this light-matter interacting system. Aside from the fact that it is always interesting to establish the connections between different approaches, our main result in Eq. (9) raises the question of whether a GS approximation remains valid for quantum open systems and/or stronger light-matter coupling strengths. For example, photon loss from the cavity is a ubiquitous deleterious effect in experimental set ups. These subjects merit considerably further studies, motivated by our work.

Conclusions.— We link directly accessible microwave observables to quantum matter correlations featuring topological phase transitions. By resorting to a GS description for the photon sub-system, a fact that turns out to be well supported by numerical DMRG calculations, we found a simple but powerful relation between the cavity FF , single-mode quadrature amplitudes and the cavity sub-system S_R . Non-analyticities

or singularities in the latter can then be of help to characterize topological phase transitions and their connection with non-monotonic non-local correlations in a fermion chain. Moreover, the FF turns out to be a reliable measurement to detect criticality in this light-matter system. Furthermore, the topological phase can be modified with both on-site as well as hopping terms of photon-fermion interactions. By increasing the local interaction, which shifts the location of the maximum Q , it is possible to take a system with fixed chain parameters towards the most topologically protected state. Equally important, with the hopping-type interaction the topological region gains in robustness. The possibility of extracting non-local or topological information of the Kitaev chain from the photonic field itself should be highly timely given the continuous challenges to assess in a clean way Majorana features in transport experiments.

Acknowledgments.— The authors acknowledge the use of the Universidad de los Andes High Performance Computing (HPC) facility in carrying out this work. J.J.M-A, F.J.R and L.Q are thankful for the support of COLCIENCIAS, through the project “*Producción y Caracterización de Nuevos Materiales Cuánticos de Baja Dimensionalidad: Criticalidad Cuántica y Transiciones de Fase Electrónicas*” (Grant No. 120480863414) and from Facultad de Ciencias-UniAndes, projects “*Quantum thermalization and optimal control in many-body systems*” (2019-2020) and “*Excited State Quantum Phase Transitions in Driven Models - Part II: Dynamical QPT*” (2019-2020). C.T acknowledges financial support from the Ministerio de Economía y Competitividad (MINECO), under project No. MAT2017-83772-R.

-
- [1] D. Rossini and R. Fazio, *New J. Phys.* **14**, 065012 (2012).
 - [2] R. J. Lewis-Swan, A. Safavi-Naini, J. J. Bollinger, and A. M. Rey, *Nat. Commun.* **10** (2019).
 - [3] A. Elben, B. Vermersch, M. Dalmonte, J. I. Cirac, and P. Zoller, *Phys. Rev. Lett.* **120**, 050406 (2018).
 - [4] T. Brydges, A. Elben, P. Jurcevic, B. Vermersch, C. Maier, B. P. Lanyon, P. Zoller, R. Blatt, and C. F. Roos, *Science* **364**, 260263 (2019).
 - [5] A. Camacho-Guardian, R. Paredes, and S. F. Caballero-Bentez, *Phys. Rev. A* **96** (2017).
 - [6] X. Zhang, K. Zhang, Y. Shen, S. Zhang, J.-N. Zhang, M.-H. Yung, J. Casanova, J. S. Pedernales, L. Lamata, E. Solano, and K. Kim, *Nat. Commun.* **9**, 195 (2018).
 - [7] K. Baumann, C. Guerlin, F. Brennecke, and T. Esslinger, *Nature* **464**, 1301 (2010).
 - [8] K. Baumann, R. Mottl, F. Brennecke, and T. Esslinger, *Phys. Rev. Lett.* **107**, 140402 (2011).
 - [9] J. Lonard, A. Morales, P. Zupancic, T. Esslinger, and T. Donner, *Nature* **543**, 8790 (2017).
 - [10] A. Thomas, E. Devaux, K. Nagarajan, T. Chervy, M. Seidel, D. Hagenmüller, S. Schtz, J. Schachen-

- mayer, C. Genet, G. Pupillo, and T. W. Ebbesen, [arXiv:1911.01459](#).
- [11] M. Trif and Y. Tserkovnyak, *Phys. Rev. Lett.* **109**, 257002 (2012).
 - [12] M. C. Dartiailh, T. Kontos, B. Douçot, and A. Cottet, *Phys. Rev. Lett.* **118**, 126803 (2017).
 - [13] F. Schlawin, A. Cavalleri, and D. Jaksch, *Phys. Rev. Lett.* **122**, 133602 (2019).
 - [14] H. Gao, F. Schlawin, A. Cavalleri, and D. Jaksch, [arXiv:2003.05319](#).
 - [15] W. Nie, Z. Peng, F. Nori, and Y.-x. Liu, *Phys. Rev. Lett.* **124** (2020).
 - [16] P. Forn-Díaz, L. Lamata, E. Rico, J. Kono, and E. Solano, *Rev. Mod. Phys.* **91**, 025005 (2019).
 - [17] A. Frisk Kockum, A. Miranowicz, S. De Liberato, S. Savasta, and F. Nori, *Nat. Rev. Phys.* **1**, 19 (2019).
 - [18] V. Mourik, K. Zuo, S. M. Frolov, S. R. Plissard, E. P. A. M. Bakkers, and L. P. Kouwenhoven, *Science* **336**, 1003 (2012).
 - [19] S. Nadj-Perge, I. K. Drozdov, J. Li, H. Chen, S. Jeon, J. Seo, A. H. MacDonald, B. A. Bernevig, and A. Yazdani, *Science* **346**, 602 (2014).
 - [20] S. M. Albrecht, A. P. Higginbotham, M. Madsen, F. Kuemmeth, T. S. Jespersen, J. Nygrd, P. Krogstrup, and C. M. Marcus, *Nature* **531**, 206209 (2016).
 - [21] H. Zhang, C.-X. Liu, S. Gazibegovic, D. Xu, J. A. Logan, G. Wang, N. van Loo, J. D. S. Bommer, M. W. A. de Moor, D. Car, and et al., *Nature* **556**, 7479 (2018).
 - [22] F. J. Gómez-Ruiz, J. J. Mendoza-Arenas, F. J. Rodríguez, C. Tejedor, and L. Quiroga, *Phys. Rev. B* **97**, 235134 (2018).
 - [23] A. Bermudez, L. Amico, and M. A. Martin-Delgado, *New. J. Phys.* **12**, 055014 (2010).
 - [24] L. Amico, R. Fazio, A. Osterloh, and V. Vedral, *Rev. Mod. Phys.* **80**, 517 (2008).
 - [25] D. Aasen, M. Hell, R. V. Mishmash, A. Higginbotham, J. Danon, M. Leijnse, T. S. Jespersen, J. A. Folk, C. M. Marcus, K. Flensberg, and J. Alicea, *Phys. Rev. X* **6**, 031016 (2016).
 - [26] A. Y. Kitaev, *Sov. Phys. Usp.* **44**, 131 (2001).
 - [27] F. Wilczek, *Nat. Phys.* **5**, 614 (2009).
 - [28] S. R. Elliott and M. Franz, *Rev. Mod. Phys.* **87**, 137 (2015).
 - [29] S. Burton, [arXiv:1610.05384](#).
 - [30] Y. Wang, *Phys. Rev. E* **98**, 042128 (2018).
 - [31] Z.-C. Yang, T. Iadecola, C. Chamon, and C. Mudry, *Phys. Rev. B* **99**, 155138 (2019).
 - [32] N.-H. Kim, Y.-S. Shin, H.-S. Kim, J.-D. Song, and Y.-J. Doh, *C. Appl. Phys.* **18**, 384 (2018).
 - [33] O. L. Acevedo, L. Quiroga, F. J. Rodríguez, and N. F. Johnson, *Phys. Rev. A* **92**, 032330 (2015).
 - [34] O. L. Acevedo, L. Quiroga, F. J. Rodríguez, and N. F. Johnson, *New J. Phys.* **17**, 093005 (2015).
 - [35] F. J. Gómez-Ruiz, O. L. Acevedo, F. J. Rodríguez, L. Quiroga, and N. F. Johnson, *Front. Phys.* **6**, 92 (2018).
 - [36] See the Supplemental Material at url will be inserted by publisher, for details of the calculations and derivations.
 - [37] S. Sachdev, *Quantum phase transitions* (Cambridge University Press., 1998).
 - [38] S. Suzuki, J. Inoue, and B. Chakrabarti, *Quantum Ising Phases and Transitions in Transverse Ising Models*, Lecture Notes in Physics (Springer Berlin Heidelberg, 2012).
 - [39] E. Cortese, L. Garziano, and S. De Liberato, *Phys. Rev. A* **96**, 053861 (2017).
 - [40] M. Greiter, V. Schnells, and R. Thomale, *Ann. Phys.* **351**, 1026 (2014).
 - [41] U. Schollwck, *Ann. Phys.* **326**, 96 (2011).
 - [42] R. Orús, *Nat. Rev. Phys.* **1**, 538550 (2019).
 - [43] D. J. S. Al-Assam, S. R. Clark and T. D. team, “Tensor network theory library, beta version 1.2.0,” <http://www.tensornetworktheory.org/> (2016).
 - [44] S. Al-Assam, S. R. Clark, and D. Jaksch, *J. Stat. Mech.* **2017**, 093102 (2017).
 - [45] S. Gammelmark and K. Mølmer, *Phys. Rev. A* **85**, 042114 (2012).
 - [46] C.-M. Halati, A. Sheikhan, and C. Kollath, [arXiv:2004.11807](#).
 - [47] F. A. Wolf, I. P. McCulloch, and U. Schollwöck, *Phys. Rev. B* **90**, 235131 (2014).
 - [48] J. J. Mendoza-Arenas, F. J. Gómez-Ruiz, M. Eckstein, D. Jaksch, and S. R. Clark, *Ann. Phys. (Berlin)* , 1700024 (2017).
 - [49] M. M. Rams and M. Zwolak, *Phys. Rev. Lett.* **124**, 137701 (2020).
 - [50] M. Brenes, J. J. Mendoza-Arenas, A. Purkayastha, M. T. Mitchison, S. R. Clark, and J. Goold, [arXiv:1912.02053v2](#).
 - [51] P. Nataf and C. Ciuti, *Nat. Comm.* **1** (2010).
 - [52] G. Vidal, *Phys. Rev. Lett.* **93**, 040502 (2004).
 - [53] S. Olivares, S. Cialdi, and M. G. Paris, *Opt. Commun.* **426**, 547552 (2018).
 - [54] D. Park, *Quant. Infor. Proc.* **17**, 147 (2018).
 - [55] M. G. Genoni and M. G. A. Paris, *Phys. Rev. A* **82**, 052341 (2010).
 - [56] M. Alexanian, *J. Mod. Opt.* **63**, 961967 (2015).
 - [57] M. Alexanian, *J. Mod. Opt.* **65**, 16 (2018).
 - [58] G. Adesso, D. Girolami, and A. Serafini, *Phys. Rev. Lett.* **109**, 190502 (2012).
 - [59] H. A. Haus, *J. Opt. B* **6**, S626 (2004).
 - [60] D. Andrews, *Photonics, Volume 1: Fundamentals of Photonics and Physics*, A Wiley-Science Wise Co-Publication (Wiley, 2015).
 - [61] C. Eichler, D. Bozyigit, C. Lang, M. Baur, L. Steffen, J. M. Fink, S. Filipp, and A. Wallraff, *Phys. Rev. Lett.* **107**, 113601 (2011).

—Supplemental Material—
**Rényi Entropy Singularities as Signatures of Topological Criticality in Coupled
 Photon-Fermion Systems**

F. P. M. Méndez-Córdoba¹, J. J. Mendoza-Arenas¹, F. J. Gómez-Ruiz^{2,1},
 F. J. Rodríguez¹, C. Tejedor³, & L. Quiroga¹

¹*Departamento de Física, Universidad de Los Andes, A.A. 4976, Bogotá, Colombia*

²*Donostia International Physics Center, E-20018 San Sebastián, Spain*

³*Departamento de Física Teórica de la Materia Condensada and Condensed Matter Physics Center (IFIMAC),
 Universidad Autónoma de Madrid, 28049, Spain*

I. MEAN FIELD APPROACH

We start by remembering the full Kitaev-cavity Hamiltonian described in the main text (MT):

$$\begin{aligned} \hat{\mathcal{H}} = & -\frac{\mu}{2} \sum_{j=1}^L \left[2\hat{c}_j^\dagger \hat{c}_j - \hat{1} \right] - t \sum_{j=1}^{L-1} \left[\hat{c}_j^\dagger \hat{c}_{j+1} + \hat{c}_{j+1}^\dagger \hat{c}_j \right] + \Delta \sum_{j=1}^{L-1} \left[\hat{c}_j \hat{c}_{j+1} + \hat{c}_{j+1}^\dagger \hat{c}_j^\dagger \right] \\ & + \omega \hat{a}^\dagger \hat{a} + \left(\frac{\hat{a}^\dagger + \hat{a}}{\sqrt{L}} \right) \left[\lambda_0 \sum_{j=1}^L \hat{c}_j^\dagger \hat{c}_j + \frac{\lambda_1}{2} \sum_{j=1}^{L-1} \left(\hat{c}_j^\dagger \hat{c}_{j+1} + \hat{c}_{j+1}^\dagger \hat{c}_j \right) \right]. \end{aligned} \quad (\text{S1})$$

Eq. (S1) can be written, under periodic boundary conditions and ignoring the quantum fluctuations from the mean value of the interacting observables, in the following way:

$$\hat{\mathcal{H}}_{\text{MF}} = \hat{\mathcal{H}}_{\text{C}} + \hat{\mathcal{H}}_{\text{K}} + L(\lambda_1 D - \lambda_0 S_z) \left[\hat{X} - x \right] + \lambda_0 L \hat{X} + 2x \left[\lambda_0 \sum_{j=1}^L \hat{c}_j^\dagger \hat{c}_j + \frac{\lambda_1}{2} \sum_{j=1}^{L-1} \left(\hat{c}_j^\dagger \hat{c}_{j+1} + \hat{c}_{j+1}^\dagger \hat{c}_j \right) \right]. \quad (\text{S2})$$

with constants and operators defined in the MT. The new form of the interaction term allows us to write the Hamiltonian, Eq. (S1), as the contribution of two independent systems corresponding to a Kitaev chain (in terms of fermionic operators) and a forced harmonic oscillator (bosonic operators), plus constant energy (fourth term in Eq. (S6)). Then the mean-field Hamiltonian can be written as $\hat{\mathcal{H}}_{\text{MF}} \approx \hat{\mathcal{H}}_{\text{C}}^{\text{MF}} + \hat{\mathcal{H}}_{\text{K}}^{\text{MF}} + \hat{\mathcal{H}}_{\text{Constant}}^{\text{MF}}$ where each term is grouped depending on the nature of the operators. Thus, the eigenstates of the Hamiltonian are just product of the chain and cavity states.

With the mean-field Hamiltonian $\hat{\mathcal{H}}_{\text{MF}}$ being identified, we proceed to describe the thermodynamics of the composed system (at finite temperature T , which later on will go to zero) by simply replacing new effective parameters in the Kitaev Hamiltonian. The coupling with the cavity produces a displacement of both the chemical potential and the hopping term in the form $\mu \rightarrow \mu_{\text{eff}} \equiv \mu - 2\lambda_0 x$ and $\Delta \rightarrow \Delta_{\text{eff}} \equiv \Delta - \lambda_1 x$, thus defining $\hat{\mathcal{H}}_{\text{K}}^{\text{MF}}$. $\hat{\mathcal{H}}_{\text{C}}^{\text{MF}}$ is the sum of all bosonic terms and $\hat{\mathcal{H}}_{\text{Constant}}^{\text{MF}}$ the remaining constant terms in Eq. (S6). Operators in each Hamiltonian commute between themselves. Consequently, the partition function, $Z = \text{Tr}(\exp(-\beta \hat{\mathcal{H}}_{\text{MF}}))$ [S1], with $\beta = 1/(k_{\text{B}}T)$ being k_{B} the Boltzmann constant, is the product of three different terms namely $Z = Z_{\text{K}} Z_{\text{C}} Z_{\text{Constant}}$.

Following the common procedure to diagonalize the Kitaev Hamiltonian through a Bogoliubov-de Gennes quasiparticle description [S2–S4] we find: $\hat{\mathcal{H}}_{\text{K}}^{\text{MF}} = \sum_k 2\omega_k \left(\hat{n}_k^\dagger \hat{n}_k - \frac{1}{2} \right)$, where \hat{n}_k is the quasiparticle fermion number in momentum space k at the first Brillouin zone. The dispersion relation is: $\omega_k(x) = \sqrt{[(\lambda_1 x - \Delta) \cos(k) - (\frac{\mu}{2} - \lambda_0 x)]^2 + \Delta^2 \sin^2(k)}$, where the cosine function represents the hopping while the term with the sine function is associated with the superconducting gap which does not get affected by the considered interactions. This results in a chain partition function as $Z_{\text{K}} = \prod_k 2 \cosh(\beta \omega_k)$. The cavity term can be diagonalized by the displacement of the bosonic field from which it is straightforward to obtain the partition function for the cavity term as well. For the constant term, the effect in the partition function is trivial. Following the product form of Z , the free energy, defined as $F = -\ln[Z]/\beta$, will be given by the addition of 3 terms: $F = F_{\text{K}} + F_{\text{C}} + F_{\text{Constant}}$.

The Eq.(1) in the main text can be recovered from the free energy as $\partial F / \partial S_z = 0$. With that replacement,

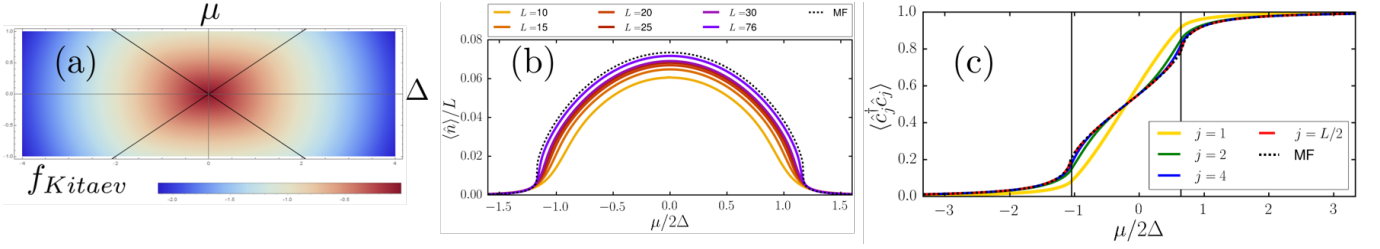


Figure S1. (a) Density plot of the Kitaev mean field free energy, $f_{\text{Kitaev}} \equiv f_{\text{Kitaev}}(x=0)$ with $\beta = 100$ as a function of μ and t . The black diagonal lines mark down the phase transition $\mu = \pm 2\Delta$. (b) Mean number of cavity photons $\langle \hat{n} \rangle$ for the hopping-like coupling. We show the results for different chain sizes compared to mean field. The parameters are $\lambda_0 = 0$, $\lambda_1 = 1$, $\Delta = 0.6\omega$ and $\omega = 1$. (c) Expected occupation at different sites in the chain. j denotes the site in the chain and $j = 1$ represents the edge site, the result for Mean Field was obtained with Eq. (1) in MT, the parameters were the same as in Fig. S2 for $L = 76$.

the free energy per site $f \equiv F/L$ results in an expression that just depends on the cavity expected value x reading as:

$$f(x) = f_{\text{Kitaev}}(x) + \omega x^2 + \lambda_0 x + \frac{1}{\beta L} \ln [1 - e^{-\beta \omega}], \quad (\text{S3})$$

where the photonic part of the ground state will be defined by the x value that minimizes the free energy. The state of the cavity will be represented by a single coherent state $|x\sqrt{L}\rangle$. This coherent state label doesn't have any imaginary part, the reason is that only the position quadrature explicitly appears in the Hamiltonian ($\hat{a}^\dagger + \hat{a}$), see Ref. [S5]. The momentum quadrature, which is directly related to the imaginary part of a coherent state (see Ref. [S6]), is regarded only implicitly in the mean number of photons $\langle \hat{a}^\dagger \hat{a} \rangle$ that appears in the Hamiltonian since an imaginary part would only add a positive energy contribution to the system as it tends to set the momentum quadrature to zero. Consequently, the mean number of photons holds $\langle \hat{a}^\dagger \hat{a} \rangle \equiv \langle \hat{n} \rangle = Lx^2$. Lastly, the free energy for the Kitaev term reads:

$$f_{\text{Kitaev}}(x) = -\frac{1}{\beta L} \sum_k \ln [2 \cosh [\beta \omega_k(x)]], \quad (\text{S4})$$

as it is shown in Fig. 1(a). Then, when the system supports super-radiance the free energy must meet the following condition for a given $x \neq 0$:

$$f_{\text{Kitaev}}(x) + \omega x^2 + \lambda_0 x - f_{\text{Kitaev}}(0) < 0. \quad (\text{S5})$$

This means that the state of the cavity controls the Kitaev chain free energy by creating an effective displacement. This control action is directly related to the mean number of photons in the cavity. It changes effectively the chemical potential and the hopping interaction, thereby driving the whole system into a less energetic state than the isolated chain would have. This shift in effective parameters is characterized by super-radiance in the cavity.

II. MATRIX PRODUCT OPERATOR REPRESENTATION

To find the whole system ground state, it is necessary to find a way to write the Hamiltonian in Eq. (S1) in a Matrix Product Operator (MPO) representation. The MPO representation can be interpreted as describing any system operator of interest as a product of matrices that only contains operators of a single site in the 1D description. For instance, any operator \hat{O} acting over a 1D system with L sites is required to be represented as $\hat{O} = \prod_{i=1}^L W^i$, where W^i is a matrix that contains operators that only act over the site i .

The Hamiltonian we are considering here describes a chain, with nearest-neighbor interactions, coupled to a global site (a single cavity field in the case of the MT). The cavity field is assumed to interact with the whole chain. The Hamiltonian can thus be generalized in the following way:

$$\hat{\mathcal{H}} = \sum_{i=1}^L h_i + \sum_{k=1}^{\alpha} \sum_{i=1}^{L-1} m_i^k n_{i+1}^k + \sum_{k=1}^{\beta} A^k \sum_{i=1}^{L-1} x_i^k y_{i+1}^k + \sum_{k=1}^{\gamma} B^k \sum_{i=1}^L z_i^k + C, \quad (\text{S6})$$

where L is the size of the chain. A^k , B^k , and C are operators that act over the global site (cavity). x_i , y_i , z_i and h_i are single-site operators (chain). α , β , and γ denote the minimum number of operators needed to conform terms corresponding to nearest-neighbor interactions in the chain (Δ); nearest-neighbor interactions in the chain with the global site (λ_1); and on-site chain terms coupled with the cavity (λ_0). It is important to note that in this way we resort to a generalized 1D system which consists of $L + 1$ sites, where the global site is located at the left end of the 1D arrangement. Denoting the site 0 as the global site, we designed an MPO for this type of Hamiltonian with W^i defined as follows:

- For $i \in [1, L - 1]$, $W^i \in T(d \times d)$ with $d = 2 + 2\beta + \gamma + \alpha$

$$W_{a,a}^i = \hat{1}, \quad a \in \{1, d\} \bigcup \{b/b = 2k + 1, \quad k \in [1, \beta]\} \bigcup \{c/c = k + 2\beta + 1, \quad k \in [1, \gamma]\};$$

$$W_{2k,1}^i = y_i^k, \quad W_{2k+1,2k}^i = x_i^k, \quad k \in [1, \beta]; \quad W_{2\beta+k+1,1}^i = z_i^k, \quad k \in [1, \gamma];$$

$$W_{2\beta+\gamma+k+1,1}^i = n_i^k, \quad W_{d,2\beta+\gamma+k+1}^i = m_i^k, \quad k \in [1, \alpha]; \quad W_{d,1}^i = h_i \text{ and } 0 \text{ for the other terms.}$$

- For the site L , $W_a^L = W_{a,1}^L$, that is the matrix will be a column vector of the corresponding matrix for the bulk.
- For the global site, site 0, we have a row vector with the form:

$$W_1^0 = C; \quad W_d^0 = \hat{1}; \quad W_{2k+1}^0 = A^k, \quad k \in [1, \beta];$$

$$W_{2\beta+k+1}^0 = B^k, \quad k \in [1, \gamma] \text{ and } 0 \text{ otherwise.}$$

In this way the Eq. (S1) is represented with the Following MPO under the Jordan-Wigner transformation:

$$W^0 = \left(\omega \hat{a}^\dagger \hat{a} + \frac{\lambda_0 \sqrt{L}}{2} (\hat{a}^\dagger + \hat{a}) \quad 0 \quad (\hat{a}^\dagger + \hat{a}) \quad 0 \quad (\hat{a}^\dagger + \hat{a}) \quad (\hat{a}^\dagger + \hat{a}) \quad 0 \quad \hat{1} \right),$$

$$W^i = \begin{pmatrix} \hat{1} & 0 & 0 & 0 & 0 & 0 & 0 & 0 \\ \sigma_x^i & 0 & 0 & 0 & 0 & 0 & 0 & 0 \\ 0 & \frac{\lambda_1}{4\sqrt{L}} \sigma_x^i & \hat{1} & 0 & 0 & 0 & 0 & 0 \\ \sigma_y^i & 0 & 0 & 0 & 0 & 0 & 0 & 0 \\ 0 & 0 & \frac{\lambda_1}{4\sqrt{L}} \sigma_y^i & \hat{1} & 0 & 0 & 0 & 0 \\ \frac{\lambda_0}{2\sqrt{L}} \sigma_z^i & 0 & 0 & 0 & 0 & \hat{1} & 0 & 0 \\ \sigma_y^i & 0 & 0 & 0 & 0 & 0 & 0 & 0 \\ \frac{\mu}{2} \sigma_z^i & 0 & 0 & 0 & 0 & 0 & -\Delta \sigma_y^i & \hat{1} \end{pmatrix}, \quad i \in [2, L].$$

$$W^L = \begin{pmatrix} \hat{1} \\ \sigma_x^L \\ 0 \\ \sigma_y^L \\ 0 \\ \frac{\lambda_0}{2\sqrt{L}} \sigma_z^L \\ \sigma_y^L \\ \frac{\mu}{2} \sigma_z^L \end{pmatrix},$$

where σ_x^i , σ_y^i and σ_z^i are the Pauli matrices for the site i .

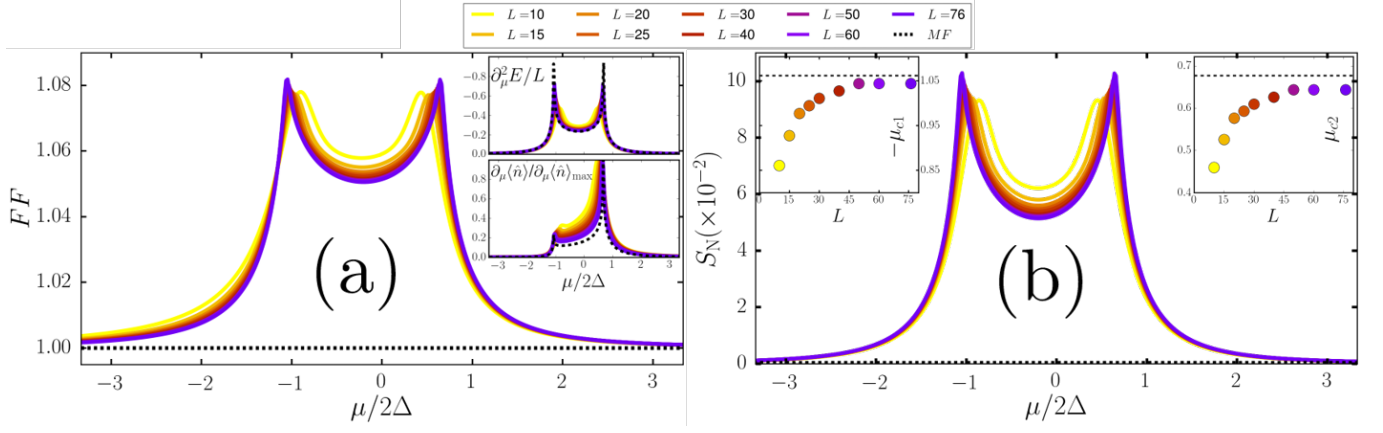


Figure S2. On-site coupling strength observables; (a) FF of the cavity. Insets: other expected values of the system that show singularities at the critical points of phase transition, each graph depicts the correspondent expected values for different sizes of the chain. The mean field (MF) results are shown by the dashed black line. Upper inset: second energy derivative with respect to $\mu/2\Delta$. Lower inset: first derivative of the number of photons, each curve is normalized with the respective maximum. (b) Von Neumann entropy of the system with a bipartition between photons and the Kitaev chain. Insets: Scaling of the critical points with the size of the chain, the mean field value is shown with the dashed line. The parameters for these plots are $\omega = 1$, $\Delta = 0.6\omega$, $\lambda_0 = 0.49\omega$ and $\lambda_1 = 0\omega$.

III. DENSITY MATRIX RENORMALIZATION GROUP VS MEAN FIELD

Our results show two second-order phase transitions in the composite photon-fermion (or Dicke-Kitaev) model, those can be identified in the upper inset of Fig. S2(a) for different sizes of the chain and the result shows a rapid convergence, as expected, to what is obtained from the mean-field scheme. For an isolated chain, with the parameters used for Fig. S2(b), the phase transition should occur at $\mu/2\Delta = \pm 1$. For a chain-cavity coupled system, in contrast, they now occur at $\mu/2\Delta = -1.04 \pm 0.02$ and 0.64 ± 0.02 . By plotting cavity observables it is possible to identify two of them that exhibit criticality. In Fig. S2(a), and its lower inset, we find that the maximum of the FF and the first derivative of the number of photons match with the critical points predicted by the second energy derivative. With the former expected value, it can be shown that the state of the cavity gets slightly farther from a coherent state as the system approaches criticality. The FF curve shares a similar shape to that of the Von-Neumann entropy (cf. Fig. S2(b)). This fact, along with the FF behavior, let us conclude that the chain and the cavity increase their entanglement at the critical points, thus driving the cavity into a super Poissonian state.

The shift of the critical points can be understood considering Eq. (S3) and the Kitaev chain free energy in Eq. (S4). This last equation, at a fixed Δ and with $\lambda_0, \lambda_1 = 0$, is a u -shaped curve with a maximum at $\mu = 0$, a curve that decays faster as we get farther from the critical point (cf. Fig. 1(a)). Then, the free energy of the whole system would allow super-radiance if μ_{eff} gets farther from the maximum in Eq. (S4) and if $-\lambda_0/\omega \leq x \leq 0$, the last condition implying that just a new $\mu_{\text{eff}} \geq \mu$ can be found. For this reason, the system joins slightly earlier in the topological phase (sweeping from $\mu < 0$ to $0 < \mu$) and leaves it highly sooner. Since the shift of the critical point is related to the light-matter coupling, the more the subsystems are interacting, the more the change of the critical value. In the left inset of Fig. S2(b), we can see that the critical points accurately converge to the result predicted by the mean-field. Slight disagreements are higher for μ_{c2} , since the cavity, and therefore correlations, play a more significant role for that parameter region because it is easier to generate radiation. Thus, the number of cavity photons acts as a control parameter that changes the chemical potential in the system's free energy. The u -shaped free energy will require x to be the minimum possible value as we get farther from the maximum to the right. As a consequence, in such a region the number of cavity photons will asymptotically approach to $n = (\lambda_0/\omega)^2$, generating what we call the asymptotically super-radiant phase in the phase diagram shown in the MT. Deep in the left region of the maximum, the free energy will require the maximum x possible; then $\langle \hat{n} \rangle$ will vanish and this behavior is considered trivial. In the transition between the non-radiant and asymptotic phases, we can find the topological phase, a phase that will be super-radiant for the cavity. Therefore, the topological phase can be recognized as the phase between peaks in the first derivative of the number of photons in the lowest inset in Fig. S2(a).

The Eq. (5) of the MT fit the numerical results with differences of about 3 orders of magnitude less than the observed value, as well as does the difference between $\langle \hat{n} \rangle$ and Lx^2 . These differences exhibit peaks at the critical points, but the order of magnitude shows the consistency of the states with mean-field results. We can observe the site dependence of that relation in Fig. 1(c) with the readings of the occupation number. The value of x for $L = 76$ is in excellent agreement with the value obtained for $\langle c_{L/2}^\dagger c_{L/2} \rangle$ (through Eq. (5) MT) and it is even quantitatively accurate for values close to the edge such as with $j = 2, 4$, but the discrepancy within the topological region is high at the edge site. Then, it is important to note that the global coupling won't provide us a direct reading of the chain state at the edge. This is because as the cavity interacts with the whole chain, the chain expected values that are extracted from the cavity do represent averaged information.

For the hopping like interaction, we find again two second-order phase transitions in the composite model. However, in this case, the phase transition is symmetrical with respect to μ . Criticality can be identified as peaks in the FF and the absolute value of the first derivative of the number of photons, similar to the λ_0 coupling case discussed above. The effect of Δ_{eff} in the free energy can be understood again considering the isolated Kitaev free energy. Regarding Δ as the independent variable, holding μ constant and using $\lambda_0, \lambda_1 = 0$, the free energy is again an u-shaped curve with a maximum at $\Delta = 0$ (cf. Fig. 1(a)). Then, x will allow super-radiance to minimize the free energy of the whole system. Eq. (5) MT holds, but again the resultant first neighbor correlations only describe correctly bulk values since the global coupling homogenizes the information of local observables.

The most remarkable result of this kind of nonlocal coupling is the behavior of the cavity as a control device. In Fig. 1(b) we observe the number of cavity photons for different values of μ , results which clearly converge to the mean-field result. Therefore, we can conclude that the expected values of the cavity can be correctly described by a coherent state, at least, for the number of photons and quadratures, but it is not enough for the FF. We can identify an abrupt jump in the number of photons at $\mu_c/2\Delta = \pm(1.14 \pm 0.01)$, for a chain of $L = 76$ sites. Following the Q value, it is at that point where the phase transition occurs, and in the super-radiant region, $-\mu_c < \mu < \mu_c$, we can find the topological phase.

IV. GAUSSIAN STATES

The mean-field analytical results provided an accurate description of the bulk values in the chain, the number of photons, and the energy of the system as a whole. However, this approximation finds flaws to take account of correlations in calculating expected values, such as the FF, and, of course, entropy values. All the information contained in a Gaussian state is coded by its covariance matrix σ :

$$\sigma = \begin{pmatrix} \langle \hat{q}^2 \rangle - \langle \hat{q} \rangle^2 & \langle \hat{q}\hat{p} + \hat{p}\hat{q} \rangle - \langle \hat{q} \rangle \langle \hat{p} \rangle \\ \langle \hat{q}\hat{p} + \hat{p}\hat{q} \rangle - \langle \hat{q} \rangle \langle \hat{p} \rangle & \langle \hat{p}^2 \rangle - \langle \hat{p} \rangle^2 \end{pmatrix},$$

and the quadrature first moments. The co-variance matrix is associated to the Gaussian parameters with the following relations [S53]:

$$\langle \hat{q}^2 \rangle - \langle \hat{q} \rangle^2 = \frac{1+2N}{2} (\cosh[2r] + \sinh[2r] \cos \phi); \quad \langle \hat{p}^2 \rangle - \langle \hat{p} \rangle^2 = \frac{1+2N}{2} (\cosh[2r] - \sinh[2r] \cos \phi);$$

$$\langle \hat{q}\hat{p} + \hat{p}\hat{q} \rangle - \langle \hat{q} \rangle \langle \hat{p} \rangle = \frac{1+2N}{2} [\sinh(2r) \sin \phi]; \quad \langle \hat{q} \rangle = \sqrt{2} \text{Re}(\alpha); \quad \langle \hat{p} \rangle = \sqrt{2} \text{Im}(\alpha),$$

with operators and parameters defined in the MT. This fundamental Gaussian information was build from DMRG ground state expected values as discussed in the MT. As it was said in Sec. , the imaginary part of $\alpha = 0$, leading to $\alpha \in \mathbb{R}$ for all parameters, then $\langle \hat{q}\hat{p} + \hat{p}\hat{q} \rangle = 0$. Now looking at the results for N, r and α the approximations $N, r \ll |\alpha|$ and $N, r \ll 1$ are justified in the analyzed parameter window. We also compared the mean number of photons obtained with the Gaussian approximation, $\langle \hat{n} \rangle = (N+1/2) \cosh[2r] + \alpha^2 - 1/2$ which under the approximations defined above is $\langle \hat{n} \rangle \approx \alpha^2$, with the obtained with DMRG, finding that they fit exactly, as can be seen in Fig.3.

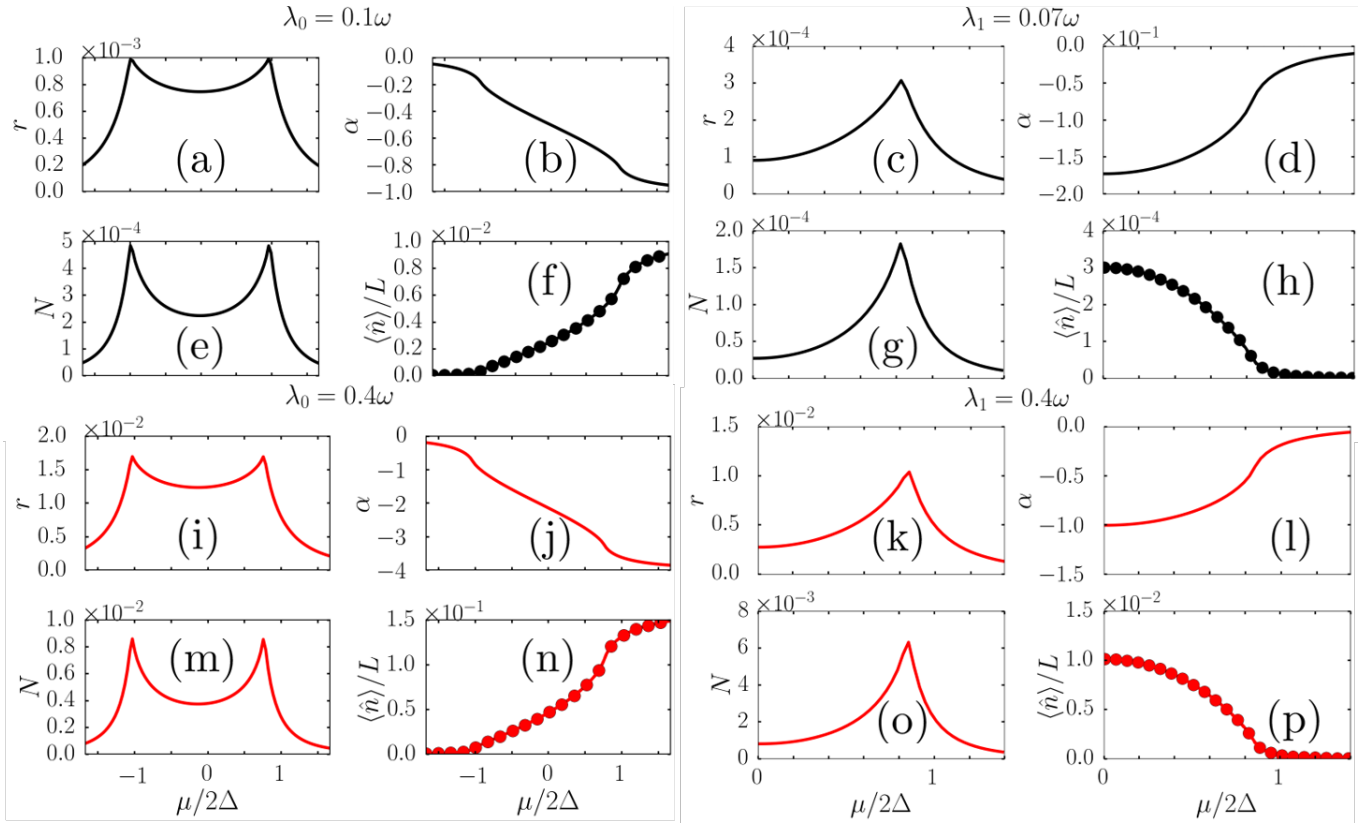


Figure S3. Gaussian parameters and number of photons : Squeezing parameter r in (a), (c), (i) and (k); coherent α parameter in (b), (d), (j) and (l); thermal N parameter in (e), (g), (m) and (o). Mean number of photons obtained with DMRG (GS) symbols (lines) in (f), (h), (n) and (p). On-site coupling strengths: (a), (b), (e) and (f) $\lambda_0 = 0.1\omega$ while (i), (j), (m) and (n) $\lambda_0 = 0.4\omega$. Hopping-like coupling strengths: (c), (d), (g) and (h) $\lambda_1 = 0.07\omega$ while (k), (l), (o) and (p) $\lambda_1 = 0.4\omega$. Other parameters $L = 100$ and $\Delta = 0.6\omega$.

-
- [S1] L. Reichl, *A Modern Course in Statistical Physics*, Physics textbook (Wiley) 2009.
[S2] S. Suzuki, J. Inoue, and B. Chakrabarti, *Quantum Ising Phases and Transitions in Transverse Ising Models*, Lecture Notes in Physics. (Springer Berlin Heidelberg) 2012
[S3] F. Wilczek, *Nat. Phys.* **5**, 614 (2009).
[S4] S. Gammelmark and K. Molmer, *New J. Phys.* **13**, 053035 (2011).
[S5] M. O. Scully and M. S. Zubairy, *Quantum Optics* (Cambridge University Press) 1997.
[S6] S. J. B. Tom Lancaster. *Quantum Field Theory for the Gifted Amateur* (Oxford University Press) 2014.